# ON THE EFFECTS OF A FINITE APERTURE ON THE INVERSE BORN APPROXIMATION

V. G. Kogan and James H. Rose

Ames Laboratory-USDOE
Iowa State University
Ames, IA 50011

## ABSTRACT

One of the most important effects of complex part geometry is that the available entrance and exit angles for ultrasound are limited. We will present a study of the Inverse Born Approximation in which we have data for incident (and exit) directions confined to a conical aperture. Modeling the direct problem by the Born Approximation, we obtained analytical results for (1) a weak spherical inclusion, and (2) a penny shaped crack (modeled by an oblate spheroid). General results are: (a) the value of the characteristic function $\gamma$ is constant in the interior of the flaw, but reduced in value; (b) the discontinuity at the boundary of the flaw occurs over the "lighted" portion of the flaw; (c) this discontinuity is contrasted by a region where $\gamma$ is negative; and (d) new non-physical discontinuities and non-analyticities appear in the reconstructed characteristic function. These general features also appear in numerical calculations which use as input strong scattering data from a spherical void and a flat penny shaped crack in Titanium. The numerical results can be straightforwardly interpreted in terms of the analytical calculation mentioned above, indicating that they will be useful in the study of realistic flaws. We conclude by discussing the stabilization of the aperture limited inversion problem and the removal of non-physical features in the reconstruction.

---

This work was sponsored by the Center for Advanced Nondestructive Evaluation, operated by the Ames Laboratory, USDOE, for the Defense Advanced Research Projects Agency and the Air Force Wright Aeronautical Laboratories/Materials Laboratory under Contract No. W-7405-ENG-82 with Iowa State University.

## 1. INTRODUCTION

A common feature of different linear inversion methods is that they involve a Fourier transform of the scattering data. The complete specification of the Fourier transform requires scattering data at all frequencies and for all directions of incidence or all directions of exit. As a rule, such complete information is not available (due to, e.g., the shape of the object containing the inhomogeneity). The problem of determining the shape of the flaw when scattering data are available for a specified set of incident and exit directions is called the finite aperture (or the limited access) problem and is the topic of this paper.

For the sake of definiteness we will couch our results in terms of the ultrasonic inverse Born Approximation [1] which holds when flaws are only weakly different from the host. Nonetheless, the general features of the results will be shown to be relevant for strongly scattering flaws such as voids and cracks and for other inversion methods such as physical optics and synthetic aperture imaging.

The structure of this paper is as follows. In the second section we review briefly the inverse Born approximation and define the aperture limited characteristic function $\gamma_a(r)$. The general form of the real part of this function is obtained in Section 3. In Section 4 we find analytically $\gamma_a(r)$ for a weak scattering uniform sphere. Next we compare our analytical results with the numerically obtained characteristic functions for a strongly scattering sphere, spheroid and flat penny shaped crack (Section 5). In the last section, we discuss our results and their connection to the general problem of determining the true characteristic function from the aperture limited $\gamma_a$.

## 2. STATEMENT OF PROBLEM

The scattering of elastic waves from defects in an otherwise isotropic homogeneous elastic medium is determined by differences in density and elastic constants of the flaw and the host, as well as by the flaw shape. For the sake of simplicity we consider here flaws which differ from the host only in acoustic impedance z. The difference $\delta z$ is assumed to be small ($\delta z/z<<1$). Then the scattering can be considered as weak and the Born approximation [2,3] can be used.

In this approximation the scattering amplitude $A(\vec{k})$ is simply related to the characteristic function $\gamma(\vec{r})$ that determines the flaw shape; by definition $\gamma(\vec{r})=1$ inside the flaw and it is zero otherwise. For the backscattering from a uniform flaw ($\delta z$=const.) this relation is given by the formulas[1]:

$$\frac{A(\vec{k})}{k^2} = \int \gamma(\vec{r}') \, e^{2i\vec{k}\cdot\vec{r}'} \, d\vec{r}' \tag{1}$$

$$\gamma(\vec{r}) = \int \frac{A(\vec{k})}{k^2} \, e^{-2i\vec{k}\cdot\vec{r}} \, \frac{d\vec{k}}{4\pi^3} \quad . \tag{2}$$

Here $2\vec{k}$ is the wave vector transfer; i.e., $\vec{k}$ is the wave vector of the backscattered wave. The definition of A chosen here includes $\delta z/z$ and other constants for convenience. The scalar form of A implies that Eqs. (1) and (2) are applicable to acoustic or longitudinal-longitudinal scattering processes. There are no essential difficulties in including transverse to transverse scattering in our scheme. The factor $(4\pi^3)^{-1}$ comes from $d(2\vec{k})/(2\pi)^3$.

The reconstruction of the flaw shape $\gamma(\vec{r})$ with the help of Eq. (2) requires knowledge of $A(\vec{k})$ at all frequencies $\omega = ck$ (c is the sound velocity) and for all directions $\hat{k}$ within the total solid angle $4\pi$. This information is never available in practice for two major reasons. The first one is that real transducers have a finite bandwidth. This difficulty can be settled by an appropriate choice of a band. With a reasonable compromise (see e.g., the discussion in Section 5) and Fig. 5 of this paper one can choose a cut-off at large k's without loosing any essential information about the flaw shape.

Another limitation stems out of obvious restrictions imposed on possible signal directions $\hat{k}$ by the experimental set-up. Usually, a cone of available k's, or "the finite aperture", constitutes less than 1/2 of the total solid angle. This means formally that only a part of the terms in the Fourier integral (2) is available to reconstruct the shape $\gamma(\vec{r})$.

We define now the aperture limited shape function $\gamma_a(\vec{r})$ as a result of integration only over the k-directions within the available finite aperture:

$$\gamma_a(\vec{r}) = \int_a \frac{A(\vec{k})}{k^2} \, e^{-2i\vec{k}\cdot\vec{r}} \, \frac{d\vec{k}}{4\pi^3} \tag{3}$$

Depending on the aperture chosen, this function may be severely distorted with respect to the shape function $\gamma(\vec{r})$ we are seeking to find. The question arises what information about the real flaw shape $\gamma(\vec{r})$ is still preserved in the $\gamma_a(\vec{r})$.

## 3. GENERAL RESULTS

Let us first express the $\gamma_a(\vec{r})$ in terms of $\gamma(\vec{r})$. Substituting Eq. (1) in the definition (3) of $\gamma_a(\vec{r})$ we obtain:

$$\gamma_a(\vec{r}) = \frac{1}{4\pi^3} \int \gamma(\vec{r}')d\vec{r}' \int_a d\vec{k}\, e^{2i\vec{k}\cdot(\vec{r}'-\vec{r})}.$$

We assume here that k varies from 0 to $\infty$; the effect of a finite k-band is briefly discussed in Section 6. The directions $k = \vec{k}/K$ are taken from the finite aperture cone (a). With the help of the notation $\mu = 2\hat{k}\cdot(\vec{r}'-\vec{r})$ we rewrite the last formula:

$$\gamma_a(\vec{r}) = \frac{1}{4\pi^3} \int_V d\vec{r}' \int_a d\hat{k} \int_0^\infty k^2 e^{i\mu k}\, dk. \tag{4}$$

Here $d\hat{k}$ is an element of the solid angle around $\hat{k}$-direction and the integral over $d\vec{r}'$ is extended over the flaw volume (V) only.

To obtain the real part of $\gamma_a(r)$ we notice that

$$\mathrm{Re} \int_0^\infty k^2 e^{i\mu k} dk = \tfrac{1}{2} \int_{-\infty}^{\infty} k^2 e^{i\mu k} dk = -\pi \frac{d^2\delta(\mu)}{d\mu^2} \tag{5}$$

Therefore,

$$\mathrm{Re}\, \gamma_a(\vec{r}) = \frac{1}{4\pi^3} \int_a d\hat{k} \int_v dV\delta''(\mu); \tag{6}$$

here $dV \equiv d\vec{r}'$ is the volume element at a point $\vec{r}'$.

To calculate the last integral we choose the coordinates with the origin at the point $\vec{r}$, where the $\gamma_a$ should be found (the point P in Fig. 1a). Let us direct one of the axes of this system along $\hat{k}$; the corresponding coordinate we denote by q. Then, with $\vec{\rho} = \vec{r}' - \vec{r}$ we have

$$\mu = 2\hat{k}\cdot(\vec{r}'-\vec{r}) = 2\hat{k}\cdot\rho = 2q \tag{7}$$

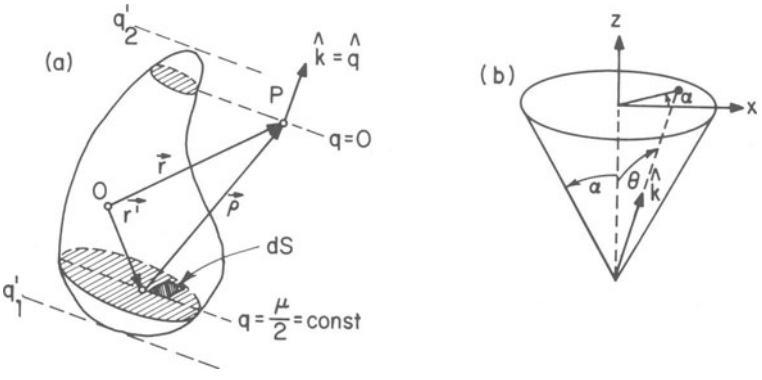


Fig. 1. (a) $P(\vec{r})$ is the "observation point" where the characteristic function $\gamma(\vec{r})$ is to be found. The shaded cross-sections are in planes normal to $\hat{k}$; dS is the plane area element. The $q'_{1,2}$ are the limits of $q' = \hat{k}\cdot\vec{r}'$. (b) The aperture cone has a half angle $\alpha$ at its vertex. The angles $\theta$ and $\phi$ are the spherical coordinates of the unit vector k: $0<\theta<\alpha$, $0<\phi<2\pi$.

The volume element in the integral over the flaw can be chosen as dV = dqdS with dS being the area element in a plant q = const. Then

$$\int_V dV\delta''(\mu) = \int dq\ ''(\mu) \int dS = \tfrac{1}{2}\left(\frac{d^2S(\mu)}{d\mu^2}\right)_{\mu=0}, \qquad (8)$$

where $S(\mu) = \int dS$ is the area of the plane $q=\mu/2$ within the flaw (see Fig. 1a). Finally, we obtain from Eqs. (6)-(8)

$$\mathrm{Re}\gamma_a(\vec{r}) = -\frac{1}{8\pi^2}\int_a d\hat{k}\,[S''(q)]_{q=0} \qquad (9)$$

This formula allows one in principle to find $\mathrm{Re}\gamma_a$ for any given flaw shape and a given aperture. If at some point $P(\vec{r})$ the plane $q = 0$ for a given $\hat{k}$ does not cross the flaw (see Fig. 1a), then $S''$ is zero and hence the direction $\hat{k}$ does not contribute in the integral (9). When this is true for all $\hat{k}$'s within the aperture a, then $\mathrm{Re}\,(r)=0$ at the point $\vec{r}$.

It turns out that the $\mathrm{Im}\gamma_a$ is less convenient for reconstruction purposes than $\mathrm{Re}\gamma_a$; recall that the imaginary part of the exact characteristic function $\gamma(\vec{r})$ is identically zero.

The result (9) can also be expressed [4] in terms of the impulse response function [5] defined as

$$R(t,\hat{k}) = \frac{1}{2\pi c} \int_{-\infty}^{\infty} A(\vec{k})\, e^{-i\omega t}\, d\omega \tag{10}$$

$(\omega=kc)$:

$$\mathrm{Re}\gamma_a(\vec{r}) = \frac{1}{\pi^2} \int_a d\hat{k}\, R\left(\frac{2\hat{k}\cdot\vec{r}}{c},\hat{k}\right). \tag{11}$$

## 4. SPHERICAL FLAW

In this case, the problem of finding the $\mathrm{Re}\gamma_a$ from Eq. (9) can be solved analytically for a finite aperture in the form of a circular cone. Let us first calculate the derivative $S''(q)$ at $q = 0$ for the sphere of a radius a. We place the origin 0 of $\vec{r}$ at the sphere center as is shown in Fig. 2a. From the definition (7) we have

$$q = \hat{k}\cdot(\vec{r}'-\vec{r}) = q' - \hat{k}\cdot\vec{r} \tag{12}$$

where $q' = \hat{k}\cdot\vec{r}'$ is the distance from the sphere center to the plane which is normal to $\hat{k}$ and contains the point $\vec{r}'$ (see Fig. 2a). The fraction of this plane inside the sphere has an area $S(q') = \pi(a^2-q'^2)$ if $|q'|<a$ and it is zero otherwise. Hence,

$$\frac{d^2S}{dq^2} = \frac{d^2S}{dq'^2} = \begin{cases} -2\pi & |q'|<a; \\ 2\pi a\,\delta(|q'|-a), & |q'|=a; \\ 0, & |q'|>a; \end{cases} \tag{13}$$

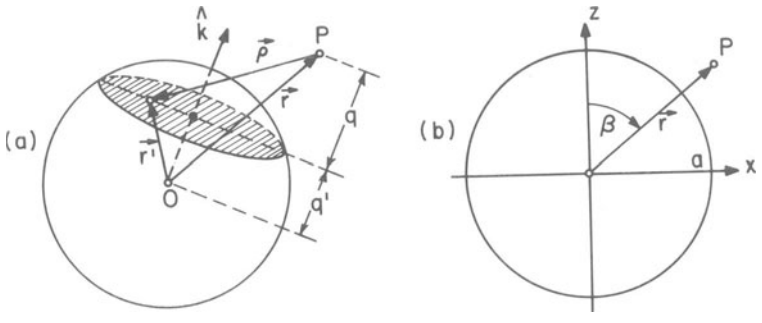


Fig. 2. (a) The characteristic function $\mathrm{Re}\gamma_a(\vec{r})$ at the point $P(\vec{r})$. The cross-section of the sphere defined by the plane $\hat{k}\cdot\vec{r}'=$ const. is normal to $\hat{k}$. (b) The definition of the polar coordinates used in the text: $z = r\cos\beta$, $x = r\sin\beta$.

where $\delta(|q'|-a) \equiv \delta(q'-a) + \delta(q'+a)$. The pre-factor of the $\delta$-function assures the correct discontinuity of $dS/dq'$ at $|q'|=a$. With the help of the step-function $\chi(q'-a)$ ($\chi$ is 1 for $q'<a$ and 0 for $q'<a$), Eq. (13) reads

$$S''(q) = -2\pi\{[\chi(q'-a)-a\delta(q'-a)]-[\chi(q'+a)+a\delta(q'+a)]\}. \qquad (14)$$

According to Eq. (9), we put here $q = 0$ or $q' = \hat{k}\cdot\vec{r}$ (see Eq. (12)). Then Eq. (9) transforms to

$$\mathrm{Re}\gamma_a(\vec{r}) = \gamma_1 - \gamma_2 \qquad (15)$$

$$\gamma_1 = \frac{1}{4\pi}\int_0^{\alpha}\sin\theta d\theta\int_0^{2\pi} d\phi[\chi(\xi)-a\,\delta(\xi)] \qquad (15a)$$

$$\gamma_2 = \frac{1}{4\pi} \int_0^{\alpha} \sin\theta d\theta \int_0^{2\pi} d\phi[\chi(\eta)+a\delta(\eta)] \tag{15b}$$

$$\xi = \hat{k}\cdot\vec{r}-a, \quad \eta = \hat{k}\cdot\vec{r} + a$$

Here $\theta$ is the angle between $\hat{k}$ and the axis z of the aperture cone, and $\alpha$ is the half angle at the cone vertex (see Fig. 1b); the angle $\phi$ is the azimuth of k within this cone. Thus, $0<\theta<\alpha$, $0<\phi<2\pi$.

Under the replacement $\vec{r}$ with $-\vec{r}$, $\xi$ goes to $-\eta$ and $\eta \to -\xi$, where $\mathrm{Re}\gamma_a$ remains unchanged. Along with the cylindrical symmetry of our problem this makes it sufficient to find $\mathrm{Re}\gamma_a$ in one quadrant of the zx-plane where z,x>0 (see Fig. 2b).

Let us deal first with $\gamma_1$ of Eq. (15a). The spherical components of $\hat{k}$ and $\vec{r}$ are $\{1,\theta,\phi\}$ and $\{r,\beta,0\}$ (see Fig. 2a), so that

$$\xi = A\cos\phi + B - a, \tag{16}$$

$$A = r\sin\beta\sin\theta = x\sin\theta,$$

$$B = r\cos\beta\cos\theta = z\cos\theta.$$

Note that both A and B are positive in the region of interest (x,z>0). The integral over $\phi$ in Eq. (15a) is evaluated using $\xi$ as the integration variable:

$$\Phi = \int_0^{2\pi} d\phi[\chi(\xi)-a\delta(\xi)] = 2\int_0^{\pi} d\phi[\ldots] =$$

$$= 2\int_{\xi_1}^{\xi_2} \frac{d\xi(\chi-a\delta)}{[A^2-(\xi-B+a)^2]^{\frac{1}{2}}} \tag{17}$$

where the limits are

$$\xi_1 \equiv \xi(\pi) = -A+B-a = r\cos(\beta+\theta)-a \tag{18}$$

$$\xi_2 \equiv \xi(0) = A+B-a = r\cos(\beta-\theta)-a \tag{19}$$

(note: $\xi_2>\xi_1$). The three different results for $\Phi$ of Eq. (17) are possible depending on where the point $\xi=0$ is with respect to the interval $(\xi_1,\xi_2)$:

$$\Phi_a = 0, \quad 0<\xi_1 \tag{20a}$$

$$\Phi_b = 2\pi, \quad \xi_2<0, \tag{20b}$$

$$\Phi_c = \pi+2\sin^{-1}\frac{a-B}{A}-2a[A^2-(a-B)^2]^{\frac{1}{2}}, \quad \xi_1<0<\xi_2 \tag{20c}$$

The integration over $\theta$ in Eq. (15a) should be performed with caution: the limits $\xi_{1,2}$ depend on the point (z,x or r,$\beta$) where $\gamma_1$ is to be found, and on the angle $\theta$ as well. In other words, the different cases (20 a,b,c) take place in different parts of the plane (z,x) as well as in different parts of the $\theta$-integration domain $(0,\alpha)$.

Let us consider first the sphere interior where r<a (the region "0" in Fig. 3a). As is seen from Eq. (19), $\xi_2<0$ here. Hence, we use Eq. (20b) in this domain to obtain:

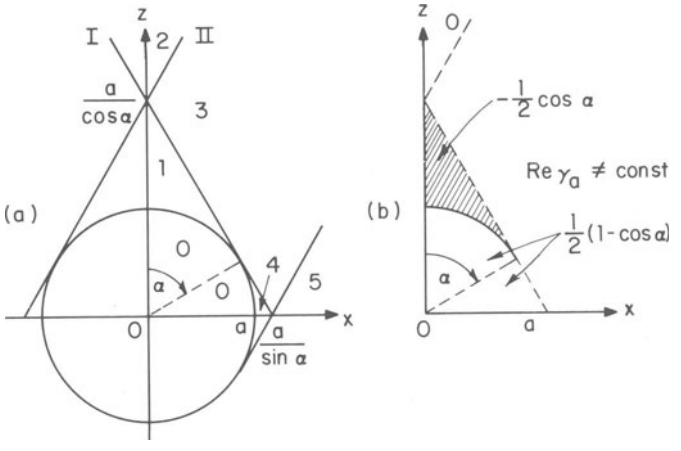


Fig. 3. (a) The straight lines I($z\cos\alpha+x\sin\alpha=a$) and II ($z\cos\alpha-x\sin\alpha=a$) divided the quadrant z,x>0 of the plane (x,z) to five domains as is indicated in the figure. (b) $\mathrm{Re}\gamma_a(\vec{r}) \neq$ const. outside of the regions where its constant values are shown explicitly.

$$\gamma_1^{(0)} = \tfrac{1}{2}(1-\cos\alpha) = \Omega_a/4\pi \tag{21}$$

where $\Omega_a$ is the solid angle of the aperture cone. We see that $\gamma_1$ is the fraction of the total solid angle within the available aperture.

Next, consider the line II of Fig. 3a defined by $r\cos(\beta+\alpha)=a$. In the region "2" above this line $r\cos(\beta+\alpha)<a$. Therefore, $r\cos(\beta+\theta)>a$ too, since $\theta<\alpha$. We see now from Eq. 18 that $\xi_1>0$ and due to Eq. (20a) we obtain

$$\gamma_1^{(2)} = 0. \tag{22}$$

Further, in the domain "4" of Fig. 3a $\beta>\alpha$ and $r\cos(\beta-\alpha)<a$. Therefore, $r\cos(\beta-\theta)<a$ is true too. This means that $\xi_2$ is negative everywhere within this domain and we obtain the same result as in the region "0":

$$\gamma_1^{(4)} = \gamma_1^{(0)} = \tfrac{1}{2}(1-\cos\alpha) \tag{23}$$

In the remaining parts of the plane (x,z) the calculation is more cumbersome because the case (20c) is involved; the detailed calculation will be given elsewhere [4].

We summarize the results in Fig. 3b. The values of $\mathrm{Re}\gamma_a$ in the regions, where it is constant, are given in the figure. The important new feature of $\mathrm{Re}\gamma_a$ is the presence of a negative constant region (the "shadow" above the solid line, or region "1" in Fig. 3a, where

$$\mathrm{Re}\gamma_a^{(1)} = -\tfrac{1}{2}\cos\alpha. \tag{24}$$

The dark inked line shows location of a discontinuity in $\gamma_1$; the jump equals to 1/2; recall that the function $\gamma(\vec{r})$ has the jump equal to 1 everywhere at the flaw surface. Still, one can state that the part of the sphere shown by the solid line in Fig. 3b (we call it "the lighted" part) is represented correctly in the aperture limited shape function.

At the dashed lines of Fig. 3b $\mathrm{Re}\gamma_a$ is continuous whereas the normal component of its gradient jumps between 0 and $\infty$. For

example, $\gamma_1^{(1)}$ is constant in the region "1" whereas in the region "3" close to the border with "1" we have $\gamma_1^{(3)} = \gamma_1^{(1)} + \text{const.}\sqrt{\varepsilon}$, where $\varepsilon$ is the distance from the line I (see Ref. 4).

The problem of a weakly scattering general ellipsoid can be reduced [4] to the problem of a sphere considered here. This reduction, however, must be accompanied by a corresponding transformation of apertures. We give here only the final results for an oblate spheroid with the symmetry axis parallel to the axis of the circular aperture cone with the half angle $\alpha$:

$$\mathrm{Re}\gamma_a^{(0,4)} = \tfrac{1}{2}\left[1 - \frac{a^2}{c^2}\tan^2\alpha\right)^{-}] \tag{25}$$

$$\mathrm{Re}\gamma_a^{(1)} = -\tfrac{1}{2}\left(1 + \frac{a^2}{c^2}\tan^2\alpha\right)^{-\frac{1}{2}} \tag{26}$$

$$\mathrm{Re}\gamma_a^{(2)} = 0 \tag{27}$$

where a and c being the major and minor semiaxes of the spheroid. The superscripts at $\gamma_a$ define different regions of the plane (x,z) as is shown in Fig. 4.

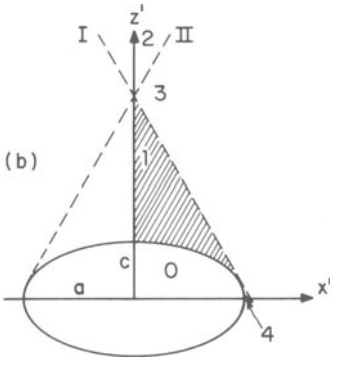


Fig. 4. The straight lines I and II divide the plane (x,z) into domains. The values of $\mathrm{Re}\gamma_a$ in the domains 0,1,2 and 4 are given the text.

## 5. COMPARISON WITH STRONGLY SCATTERING FLAWS

Our discussion up to now has been concerned with flaws which are weakly scattering. Flaws encountered in actual situations are often strongly scattering and some caution must be exercised in extrapolating the weak scattering results. Voids and cracks in elastic media are two classes of strongly scattering flaws which are of considerable interest in nondestructive evaluation. These two classes of flaws differ in that the one is volumetric while the other is not. On the other hand the scattering is defined in both cases by stress free boundary conditions at the flaw surface. In this section we will calculate numerically the aperture limited characteristic function for the case of a spherical void and for a flat penny shaped crack using the inverse Born approximation Eq. (2) where A is the true scattering amplitude and not given by Eq. (1). These results will then be compared with the analytic weak scattering results given above. For the somewhat limited comparison made, we will show that quite good agreement is found for the "lighted" region of the flaw. For the "unlighted" portion of the flaw substantial differences are expected.

The numerical evaluation starts with Eq. (3), which holds also in the strong scattering case. We consider first the sphere case. As in preceding sections, the aperture is a circular cone with the z axis and the half angle $\alpha$. The symmetry of the problem allows an analytic integration in Eq. (3) over the $\hat{k}$'s azimuthal angle $\phi$. We find

$$\gamma_a(\vec{r}) = -\frac{1}{2\pi^2}\int_0^{\infty} dk \int_0^{\alpha} d\cos\theta\, A(\vec{k}) Jo(2kr\cos\beta\cos\theta) e^{-2ikr\sin\beta\sin\theta} \quad (28)$$

Here $Jo(x)$ is the Bessel function and we used the notations $\vec{k} = \{k,\theta,\phi\}$, $\vec{r} = \{r,\beta,0\}$ in the spherical coordinates with z as the polar axis. The scattering amplitude $A(\vec{k})$ was obtained by numerically evaluating the Ying-Truell [6] series solution for scattering from a spherical void in an otherwise homogeneous, isotropic elastic medium. The Ying-Truell result is based upon the fact that the elastic wave equation separates for spherical symmetry and that the internal and scattered fields can, therefore, be expressed as an expansion over the vector spherical harmonics. The host material was chosen to have characteristics of Ti structural alloys for definiteness. The amplitude $A(\vec{k})$ was calculated for $0.1<ka<10$ and for 5° increments of $\theta$ from 0 to $\alpha$. These values of A were then substituted into a discretized version of Eq. (28) and the sums performed. For $ka>10$ we assumed that $A(k) = 0$. This latter choice results in Gibbs' phenomena (ringing) in the reconstructed characteristic function.

The numerical results for the function $\mathrm{Re}\gamma_a(r,\beta)$ (see Fig. 2b for the definition of $\beta$) are shown in Fig. 5 by the crosses for $\beta = 0°$, $15°$ and $30°$. The thin curves connect the crosses to visualize the Gibbs' phenomenon.

The inked solid lines in Fig. 5 are the analytical results obtained for a weak scattering sphere in Section 4. The aperture cone in all cases has the half angle $\alpha = 50°$. The weak scattering $\mathrm{Re}\gamma_a$ for $\beta = 0$ (z axis of Figs. 2b and 3b) is given by Eqs. (22-24). To find $\mathrm{Re}\gamma_a$ for $\beta \neq 0$ one uses Eqs. (23), (25) and Ref. 3. Both analytical and numerical results are normalized so that the characteristic functions for $r<1$ have the same value on the average. One can see that the agreement between the two is quite satisfactory if the extraneous Gibbs' ringing is ignored.

In Section 4 it has been shown that at the x-axis (see Fig. 3) the region where $\mathrm{Re}\gamma_a$ is constant is somewhat extended with respect to the real sphere interior. The upper boundary of this region is given by $x_{max} = 1/\sin 50° \cong 1.3$. This extension is clearly seen in Fig. 6 where the numerical results for $\mathrm{Re}\gamma_a$ are shown for $\beta = 90°$ (x-axis of Fig. 3).

We should note here that being satisfactory in reproducing the location of the flaw surface, the absolute value of $\mathrm{Re}\gamma_a$ obtained for a weakly scattering sphere, does not match $\mathrm{Re}\gamma_a$ found numerically for a strong scattering void. For example, at $\beta = 90°$, $|\mathrm{Re}\gamma_a|_{strong}$ is about 1/2 of $|\mathrm{Re}\gamma_a|_{weak}$. This discrepancy rapidly increases for $\beta>90°$ and agreement falls altogether for $\beta>130°$.

Figure 7 shows the $\mathrm{Re}\gamma_a$ for an oblate spheroidal void in Ti with the semiaxes ratio $c/a = \frac{1}{2}$. The reconstruction is done along the z axis of Fig. 4. The half angle of the aperture cone is 45°. The weak scattering analytical result shown by the solid inked line, is obtained from Eq. (25), (26) and (27).

The characteristic function was also numerically evaluated for the flat penny shaped crack with a conical aperture about the axis of symmetry. The numerical scattering amplitude used to evaluate Eq. (28) were provided by J. Opsal [7]. He calculated $A(\hat{k})$ using the method of optimal truncation (a T-matrix like approach) introduced by W. Visscher [8]. Again, $A(\hat{k})$ was evaluated in 5° increments of $\beta$ and for $0.10<ka<10$ in steps of 0.10. The characteristic function in this case was obtained by taking $|\gamma(\hat{r})|$ in Eq. (28). The absolute value is introduced in the inverse Born evaluation of cracks due to the difference between volumetric and areal flaws. The rather surprising result of the numerical evaluation is that the reconstructed shape is not affected at all by the presence of this particular aperture. The magnitude of the reconstructed characteristic function depended on the solid angle included by

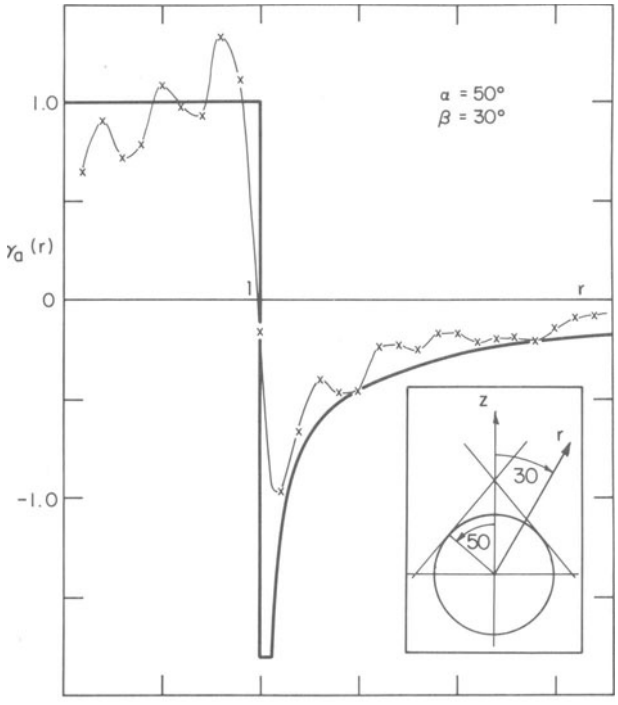


Fig. 5. The analytic weak scattering results for $\mathrm{Re}\gamma_a(r)$ are shown by the solid inked line. The crosses are the numerical results for the strong scattering void in Ti. The cases (a), (b), (c) correspond to the reconstruction directions = 0°, 15°, 30°, respectively, as is shown in the inserts.

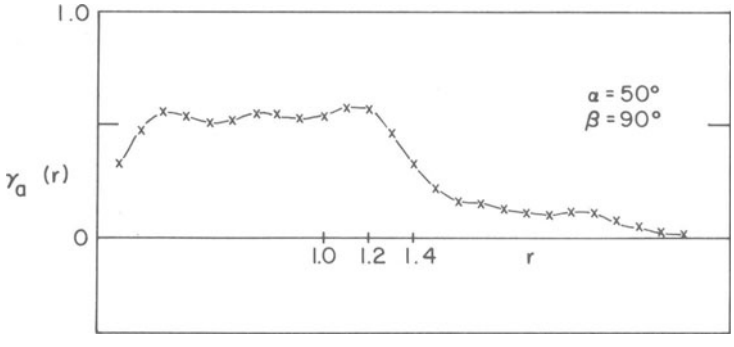


Fig. 6. The strong scattering numerical results for a spherical void in Ti in the equatorial plane normal to the aperture cone axis. For the weak scattering sphere the region of a constant $\mathrm{Re}\gamma_a(r)$ is extended up to $\tilde{}1.3$ of the real radius.

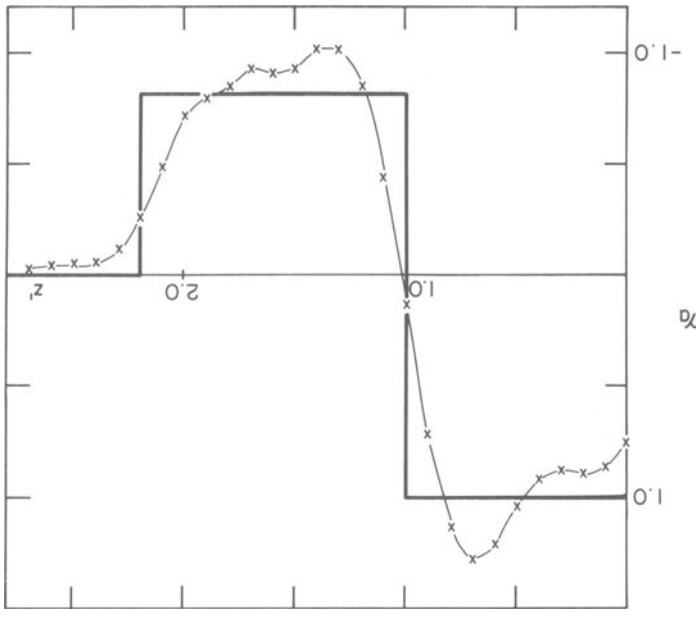


Fig. 7. The analytic weak scattering results for $\mathrm{Re}\gamma_a$ of the 2:1 oblate spheroid are shown by the solid inked line along the axis z' of the aperture cone. The crosses are the numerical results for the void in Ti of the same shape.

the aperture. These same features appear in the weak scattering reconstruction of the last section, if we model a penny shaped flaw by an oblate spheroid with major axis a and minor axis c→0. In that case, using the notation of the last section we find from Eqs. (25) and (26)

$$\gamma_1^{(0,4)} = \tfrac{1}{2} \qquad \gamma_1^{(1)} = \gamma_1^{(3)} = 0 \tag{29}$$

Also, as c→0 region 4 shrinks down to zero area and disappears. Hence, $\mathrm{Re}\gamma_a(\vec{r})$ becomes coincident with the flaw. That is

$$\mathrm{Re}\gamma_a(\vec{r}) = \tfrac{1}{2}\,\gamma(r)$$

This result resembles the aperture limited characteristic function found for the flat crack since we recover the exact characteristic function (to within a constant factor) in both cases. However,

note that $\gamma_a$ given in Eq. (29) is independent of the aperture angle. This is unlike the case of the flat strongly scattering crack where $\gamma_a(\vec{r})$ depends essentially on the aperture angle.

## 6. DISCUSSION

Within a broader context our results serve two genera purposes. First by examining $\gamma_a(\vec{r})$ for weak scattering flaws (defined by a characteristic function) we lay the basis for establishing the form of the regularization needed. Secondly, we have obtained a close connection between the weak scattering $\gamma_a(\vec{r})$ and the aperture limited characteristic functions of the strongly oblate spheroidal void and to a lesser degree of the penny shaped flat crack. Thus, (1) any methods developed to regularize the inversion of weak flaws can be extrapolated for use with crack and voids; (2) the weak scattering $\gamma_a(\vec{r})$ can be used directly to regularize the strong scattering, e.g., fitting the strong scattering $\gamma_a$ to the weak scattering result over the "lighted" surface. These possibilities are being currently investigated.

Two particular features of our results require highlighting and some further discussion. First, we have found that for sharp aperture function (i.e., either 1 or 0) unphysical non-analytic features appear in the reconstruction. For example, in the reconstruction of the spherical flaw there is a discontinuity in the characteristic function on z-axis at $z = a/\cos\alpha$. Off the z-axis the function is continuous, but at certain boundaries the slope of $\gamma_a(\vec{r})$ has an infinite discontinuity. These features contain high frequency components of the scattering amplitude. They cannot be gotten rid of simply by going to higher and high frequencies.

Thompson, Rose and Lakin [9] have shown that the synthetic aperture and other practical ultrasonic imaging methods can be derived within the context of the inverse Born formalism. Consequently, due to their high frequency content, the non-physical surfaces predicted by our treatment will be seen in these imaging methods also. We hasten to add that practically they can probably be ameliorated to some degree by apodizing the aperture function (i.e., requiring it to go to smoothly to zero at its limit, rather than dropping abruptly to zero). Another question still being answered is whether the "ghost" singularities can be used to extract an additional information on the flaw shape.

Also, the connection between the weak and strong scattering results needs further discussion. The agreement between $\gamma_a$'s for the classes of flaws considered seems somewhat startling. However, for a wide class of voids the inverse Born approximation has been shown [10] to exactly determine their size, shape and orientation. This result stems from the fact that the time domain Born approximation accurately describes the initial part of the singular structure

of the impulse response function. The singularities are due the first collison of the incoming pulse with the flaw's surface. It has been shown that these singularities determine the discontinuities at the boundary of the characteristic function. The appearance of non-analytic features in $\gamma_a(\vec{r})$ also depends on these singularities as can be seen by examining our analytic integrations in detail. A comparison of the strong and weak scattering results could be constructed on this basis. As an approximate preliminary starting point, it would be of considerable interest to obtain finite aperture results using the inverse Born approximation for voids whose scattering amplitude is modeled by the Kirchhoff (physical optics) approach.

In summary, we have developed a method for calculating the finite aperture characteristic function for weakly scattering flaws within the inverse Born approximation. Analytical results for $\gamma_a(\vec{r})$ were obtained for a spherical flaw with an aperture described by a right circular cone. These results also allow the solution for the case of ellipsoidal flaws with an aperture described by a particular elliptical cone. The finite aperture is found to result in non-physical singularities of the characteristic function. We then compared these weak scattering results to $\gamma_a(\vec{r})$ calculated numerically for a spherical void, an oblate spheroid and a flat penny shaped crack. Surprisingly, good agreement between the two methods was found for the "lighted" portion of the flaw's surface. In the discussion we pose the general problem of determining the true characteristic function from an aperture limited reconstruction and the connection of our results to this problem.

REFERENCES

1. J. H. Rose and J. A. Krumhansl, J. Appl. Phys. 50(4), 2941 (1979).
2. J. E. Gubernatis, E. Domany and J. A. Krumhansl, J. Appl. Phys. 48, 2804 (1977); and J. E. Gubernatis, E. Domany, J. A. Krumhansl and M. Huberman, Material Science Center, Cornell University Report 2654 (1975).
3. A. K. Mal and L. Knopoff, J. Inst. Math Its Appli: 3, 376 (1967).
4. V. G. Kogan and J. H. Rose, submitted to J. Acoust. Soc. Am.
5. J. H. Rose and J. M. Richardson, J. of Non-Destructive Evaluation, in press.
6. C. F. Ying and R. Truell, J. Appl. Phys. 27, 1086 (1956).
7. J. L. Opsal, Proc. of the DARPA/AFML Review of Progress in NDE, Sixth annual report, 292 (1980).
8. W. M. Visscher, J. Appl. Phys. 51, 825 (1980), and J. Appl. Phys. 51, 835 (1980).
9. R. B. Thompson, K. M. Lakin and J. H. Rose, Proc. of IEEE Ultrasonics Symposium 1, 930 (1981).
10. J. H. Rose and J. L. Opsal, these proceedings.

ACKNOWLEDGEMENTS

We would like to thank J. L. Opsal for providing us with numerical tabulation of his results.

DISCUSSION

R.C. Addison (Rockwell International Science Center): I was trying to understand from your talk how it contrasted with the talk that John Richardson gave in the previous session on looking at flaws with unknown boundaries. He basically took two noiseless wave forms only and then he reconstructed the flaw, which is a finite aperture technique also. Could you contrast what you were doing with what he's doing?

V.G. Kogan (Ames Laboratory): What we are doing is following up as fully as we can on the deterministic consequences of the inverse Born, and what John is doing is building a priori information to stabilize the lack of data. We are taking no a priori information into account in what we are doing, and our intent is to see what you can do in principle with the deterministic algorithm. In that way, when it comes to the point of building a probablistic inversion algorithm, you know what you have leverage on and what you don't. It's very important, in fact, it's absolutely crucial in the real world, to use a priori information to stabilize the inversion, and this talk is designed to be input to that development.